biAb Mediated Restoration of the Linkage between Dystroglycan and Laminin-211 as a Therapeutic Approach for α-Dystroglycanopathies

Nathan Gumlaw,[1,2] Leila M. Sevigny,[1,2] Hongmei Zhao,[1] Zhengyu Luo,[1] Dinesh S. Bangari,[1] Elizabeth Masterjohn,[1] Yangde Chen,[1] Barbara McDonald,[1] Maureen Magnay,[1] Tara Travaline,[1] Takako Yoshida-Moriguchi,[1] Wei Fan,[1] David Reczek,[1] James E. Stefano,[1] Huawei Qiu,[1] Christian Beil,[1] Christian Lange,[1] Ercole Rao,[1] Michael Lukason,[1] Elizabeth Barry,[1] William H. Brondyk,[1] Yunxiang Zhu,[1] and Seng H. Cheng[1]

[1]Sanofi, Framingham, MA 01701-9322, USA

Patients with α-dystroglycanopathies, a subgroup of rare congenital muscular dystrophies, present with a spectrum of clinical manifestations that includes muscular dystrophy as well as CNS and ocular abnormalities. Although patients with α-dystroglycanopathies are genetically heterogeneous, they share a common defect of aberrant post-translational glycosylation modification of the dystroglycan alpha-subunit, which renders it defective in binding to several extracellular ligands such as laminin-211 in skeletal muscles, agrin in neuromuscular junctions, neurexin in the CNS, and pikachurin in the eye, leading to various symptoms. The genetic heterogeneity associated with the development of α-dystroglycanopathies poses significant challenges to developing a generalized treatment to address the spectrum of genetic defects. Here, we propose the development of a bispecific antibody (biAb) that functions as a surrogate molecular linker to reconnect laminin-211 and the dystroglycan beta-subunit to ameliorate sarcolemmal fragility, a primary pathology in patients with α-dystroglycan-related muscular dystrophies. We show that the treatment of LARGE^myd-3J mice, an α-dystroglycanopathy model, with the biAb improved muscle function and protected muscles from exercise-induced damage. These results demonstrate the viability of a biAb that binds to laminin-211 and dystroglycan simultaneously as a potential treatment for patients with α-dystroglycanopathy.

INTRODUCTION

α-dystroglycanopathy is the collective term for a clinically and genetically heterogeneous group of muscular dystrophies with the biochemical hallmark of decreased or absent specific O-linked glycosylation on α-dystroglycan (αDG) due to genetic mutations in one of 18 genes identified thus far.[1–4] The hypoglycosylation of specific O-linked glycan on αDG results in diminished binding to its ligands in the extracellular matrix, including laminin-211, agrin and perlecan in muscles, neurexin in the brain, and pikachurin in the eye. These aberrations lead to clinical manifestations in muscles, the CNS, and the eye. Patients with severe α-dystroglycanopathy subtypes, such

as Walker-Warburg syndrome (WWS), muscle-eye-brain disease (MEB), and Fukuyama-type congenital muscular dystrophy (FCMD)[5,6] are typically diagnosed at birth or within a few months of life. These patients develop generalized hypotonia, developmental delays, mental retardation due to brain structural malformations, and eye abnormalities. In contrast, patients with limb-girdle muscular dystrophy (LGMD) typically acquire ambulation but develop muscle weakness in their early teens and become wheelchair bound in early or late adulthood.[7–9] Due to the lack of a strict correlation between genotype and phenotype, these diseases were recently reclassified into four subtypes:[2,10] (1) forms with congenital-onset weakness and severe structural brain abnormalities (WWS, MEB, and FCMD); (2) forms with congenital-onset weakness with brain involvement ranging from absent to moderate (congenital muscular dystrophy types 1C [MDC1C] and 1D [MDC1D]); (3) forms with later-onset limb-girdle weakness associated with mental retardation and microcephaly but without structural brain defects (LGMD type 2K [LGMD2K]); and (4) the mildest variants with no brain involvement (LGMD type 2I [LGMD2I]).

DG is a component of the dystrophin-associated glycoprotein complex (DGC), which primarily serves to link the extracellular matrix to the intracellular cytoskeleton, conferring sarcolemma stability during muscle contraction.[11–13] α- and βDGs are transcribed from the same gene (*DAG1*) and are generated by post-translational cleavage of the gene product to produce a transmembrane segment (βDG) and an extracellular, non-covalently associated protein (αDG), which is heavily O-glycosylated.[14] An important feature of this glycosylation, the mechanism of which was recently elucidated,[3,4] is the unique O-linked glycans (matriglycan) that is modified by the
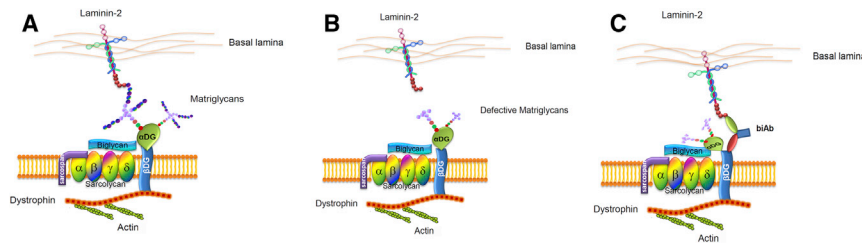
Figure 1. Illustrative Representations of the Dystroglycan Complex and Therapeutic Bispecific Antibody Approach

(A) In normal muscle, laminin-211 binds to αDG via the O-linked glycans on αDG. (B) Lack of O-linked glycans on αDG results in disconnection of laminin-211 from αDG, causing α-dystroglycanopathy. (C) An engineered biAb recognizing the laminin-211 LG4/5 domain and the ECD of βDG is proposed to restore the linkage between laminin-211 and βDG in patients with α-dystroglycanopathy. This approach acts independently of the O-linked glycans on αDG.

xylose-glucuronic acid repeats by LARGE[15] that endow αDG with ligand-binding activity.[16]

The genetic heterogeneity of α-dystroglycanopathy and the rarity of each individual subtype pose a significant challenge to developing a single treatment that would benefit all the subtypes. Both αDG (via the matriglycan) and integrin α7β1 bind to laminin-211 in the basal lamina of skeletal muscles and contribute to force production.[17] However, most of the mechanical support for sarcolemma integrity appears to be provided by the binding of laminin-211 in the basal lamina to αDG on the sarcolemma. Hence, conceptually, replacing the non-functional hypoglycosylated αDG in α-dystroglycanopathy with a functional mimic to restore the linkage between laminin-211 and the sarcolemma may serve as a therapeutic (i.e., protein replacement) for this patient population. That protein replacement may be viable was illustrated by the demonstration that local injection of purified matriglycan O-glycosylated αDG[17] into the muscles of LARGE[myd] mice conferred a measure of protection to the sarcolemma from laser-induced damage. However, when the matriglycan-glycosylated αDG was injected systemically, very little change was noted in muscle tissues, presumably due to rapid clearance by the mannose or asialoglycoprotein receptors on the cells in the reticuloendothelial system. To overcome this obstacle, we elected to develop a bispecific antibody (biAb) engineered to bind simultaneously both laminin-211 and DG to serve as a surrogate linker that connects the basal lamina to the sarcolemma. Importantly, such an approach, if successful, should be applicable to treat several subsets of α-dystroglycanopathy patients. Here, we show that administering biAbs with this functionality into LARGE[myd-3J] mice (a model of α-dystroglycanopathy) protected the animals from exercise-induced muscle damage and, consequently, improved muscle function.

RESULTS

Development of biAbs Targeting Laminin-211 and βDG

The dystrophin-associated glycoprotein complex links the intracellular cytoskeleton to the basal lamina in muscles.[13] Figure 1A depicts the key components of the DGC that create this linkage. βDG, the transmembrane protein component of DG, is positioned centrally in the DGC. Intracellularly, βDG confers mechanical support through its association with dystrophin to connect the sarcolemma with actin filaments. Extracellularly, together with the sarcoglycans and biglycan,[18,19] βDG associates with αDG to bind the basal lamina via its matriglycan with laminin-211. Because the integrity of skeletal muscle

cell sarcolemma requires both intra- and extracellular support, a defect in any one of the DGC components frequently leads to muscular dystrophy;[12,20] for example, dystrophin defects play a role in the development of Duchenne muscular dystrophy,[21] and sarcoglycan defects play a role in the development of sarcoglycanopathies.[22] In αDG-related muscular dystrophies, the link between laminin-211 and αDG is disrupted due to a deficiency in O-linked matriglycan on αDG (Figure 1B). To address this loss of function, we envisioned the development of a biAb designed to concurrently bind laminin-211 and DG and thereby act as a surrogate of the normal function of matriglycan on αDG. Since α-dystroglycanopathies may include a secondary deficiency in αDG levels, we reasoned that a biAb capable of recognizing laminin-211 and βDG rather than αDG might restore the linkage to a greater extent (Figure 1C). The spatial distance between βDG and laminin-211 was also anticipated to be a consideration for optimal DGC function. Providentially, the distance between the sarcolemma and laminin-211 is reportedly in the ~100-Å range,[17] which approximates that of biAbs that can span up to 150 Å.

Laminin-211 comprises the three subunits α2, β1, and γ1; hence, its designation as laminin-211.[23,24] The α2 subunit contains five laminin-globular (LG) domains at its C terminus that participate in binding to different extracellular molecules, such as sulfatides, integrin α7β1, and heparin;[25] the fourth and fifth LG domains (LG4/5) bind αDG via the matriglycan.[26] To minimize the potential interference of the biAb with the physiological associations between other LG domains and their respective binding partners, we elected to use the LG4/5 domains as the target antigens for the proposed biAb. Alignment of the human and mouse laminin-α2 LG4/5 protein sequences indicated that they shared a sequence identity of approximately 88% and that the identity between the human and mouse sequences of the extracellular domain (ECD) of βDG (96 amino acids) was 86%. Thus, it was conceivable that we could generate Abs that cross-reacted with both human and mouse laminin-α2 and βDG, obviating the need to develop two sets of Abs that separately recognized human and mouse targets. To this end, human and mouse laminin-α2 LG4/5 and the ECD of βDG were expressed in HEK293 cells, purified, and then used to generate hybridomas. To ensure that the Abs could recognize the native conformations of the epitopes, correct folding of LG4/5 was confirmed by binding to heparin.[25] Monoclonal antibodies (mAbs) to laminin α2 chain and βDG were identified and characterized using a variety of assays (Figures S1A–S1E) to ensure that they bound their respective targets with
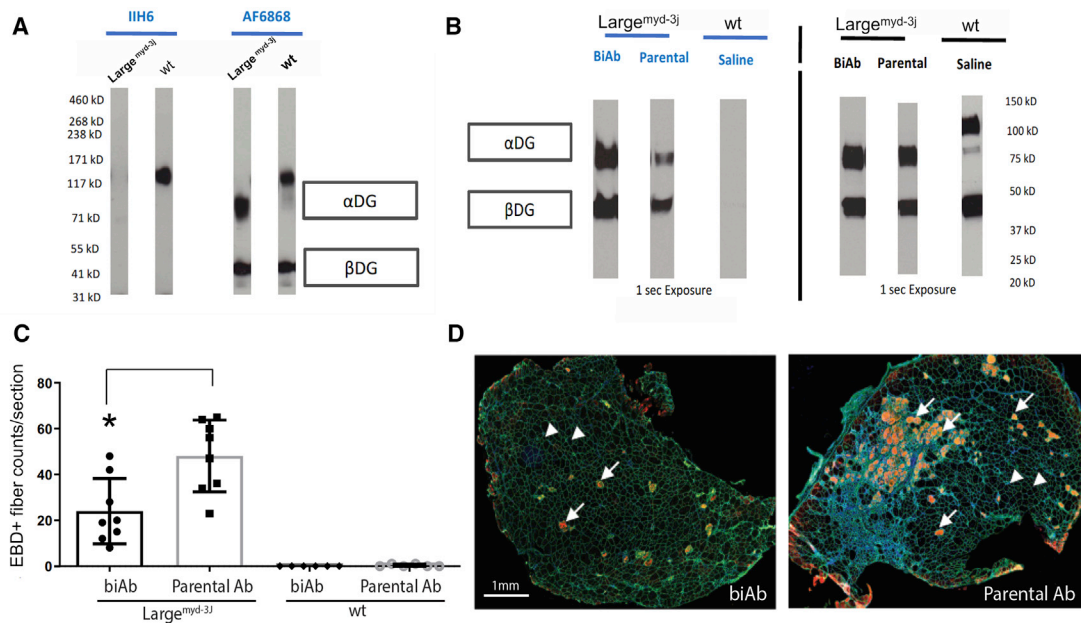
Figure 2. Localized Intramuscular Injection of the biAb into LARGE^{myd-3J} Mice Protected TA Muscles from Exercise-Induced Damage

(A) Muscle lysates of non-treated LARGE^{myd-3J} and wild-type mice show the lack of glycosylation of αDG in the LARGE mice by a IIH6-specific antibody and with a polyclonal antibody recognizing both αDG and βDG. (B) Muscle lysate IP from biAb, parental-Ab-, or saline-treated animals shows that biAb treatment does not disrupt the dystroglycan complex as shown by pulldown with the *in vivo* bound antibody (left panels) or a βDG antibody that has a different epitope than the treatment (right panels; clone 43DAG1/8D5). (C) Summary of EBD-positive fiber counts in biAb- and parental-Ab (control)-treated TA muscles. (D) Representative muscle sections of biAb- and parental-Ab-treated TA muscles. Arrows indicate EBD-positive fibers (orange fibers), and arrowheads represent Ab staining at the sarcolemma (green). Statistical analysis was performed using Student's t test; *p < 0.05. n = 8 animals per group, 6 sections at different planes were assessed per TA. Images were taken at 10× magnification.

the desired properties. The resulting mAbs positively stained unfixed frozen sections of human, mouse, and cynomolgus monkey muscle tissues, indicating that they recognized their respective targets in the native state (Figure S1C).

For an initial demonstration of proof of concept, the V_H and V_L sequences of the selected anti-laminin-211α and anti-βDG ECD mAbs were used to engineer biAbs in the tetravalent bispecific tandem immunoglobulin (Ig) (TBTI) format[27] using mouse Fc as a backbone (Figure S2A). To ensure that consequent binding of the Ab to the sarcolemma or basal lamina would not induce activation of effector cells or the complement pathway, the effector function of the Fc was silenced by introducing deltaAB mutations.[28] The biAbs were expressed in HEK293 cells, purified, and extensively characterized to verify that they retained the binding properties of the parental mAbs. We showed that the biAbs retained binding activity, albeit at a ∼10× reduced affinity to laminin-211 than the parental mAb (Table S1). Sandwich ELISA and sequential surface plasmon resonance (SPR) assays confirmed that the biAbs could engage both LG4/5 and βDG concurrently (Figures S2B and S2C). However, sequential SPR binding assays again revealed a reduction in the binding affinity of the anti-laminin-211 Ab in the TBTI biAb format with an inner V_H/V_L configuration (Figure S2B, arrowheads). This suggested that steric hindrance in the inner complementarity-determining regions may have impaired antigen binding, as predicted by crystal structure modeling.[27]

Local Intramuscular Injection of the biAb Protects the Tibialis Anterior Muscle from Exercise-Induced Damage

To evaluate whether the biAb (recognizing anti-laminin-211 and βDG) exhibited the desired function *in vivo*, we used the LARGE^{myd-3J} mouse model of α-dystroglycanopathy (Jackson Laboratory; LARGE^{myd-3J /GrsrJ}, stock #008581). The LARGE^{myd-3J} mouse has a hypomorphic mutation in *Large* (like-glycosyltransferase) that leads to a loss in *Large* expression, consequent reduced O-linked IIH6-positive matriglycans on αDG, and an ability to bind laminin-211 (in a laminin-overlay assay) and thereby render the myofibers susceptible to contraction-induced damage. LARGE is the xylose-glucuronic acid dual glycosyltransferase critical for the addition of the xylose-glucuronic acid disaccharide repeats responsible for ligand binding.[15] This reduction in glycosylation was observed in muscle lysates of LARGE^{myd-3J} mice when compared to wild-type mice using the glycosylation-specific IIH6 antibody (Figure 2A). Both αDG and βDG were also evident in the muscle lysates of wild-type and LARGE^{myd-3J} mice, with the latter showing a shift in the size of αDG reflecting a loss in glycosylation (Figure 2A). Phenotypically, this mouse model resembles a severe form of LGMD2I or FCMD in humans, with early-onset muscular dystrophy as well as eye, neuromuscular junction, and CNS abnormalities (Figure S3). When treated with the biAb, the dystroglycan complex was not disrupted as observed in immunoprecipitation assays of muscle lysates from mice that had been treated with the biAb, or the parental Abs (Figure 2B).
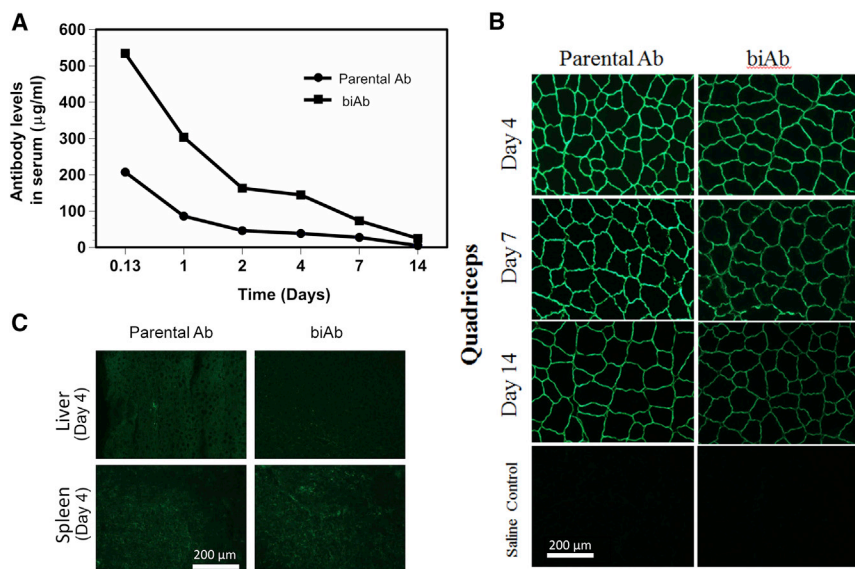
Figure 3. Biodistribution of Abs *In Vivo*

(A) Concentration of the parental Abs and biAb in serum after a single dose of the biAb (30 mg/kg) or a mixture of the parental Abs (15 mg/kg for each mAb). The half-life of the parental Abs and biAb were 83.45 h and 103.03 h, respectively. (B) Tissue biodistribution of the parental Abs and biAb in a representative muscle (quadriceps) at days 4, 7, and 14. Abs (both parental and biAb) were still clearly detectable at day 14 and were localized at the sarcolemma/basal lamina. Although the imaging was not quantitative, the tissue half-life of the Abs appeared to be greater than that in the blood. (C) Lack of staining of either the parental Abs or the biAb in non-target tissues (liver and spleen) at day 4. n = 3 animals for each time point.

sion) to assess biodistribution and *in situ* stability. As shown in Figure 3A, both the parental Abs and the biAb were still detectable in blood on day 14, albeit at low levels, with a half-life of approximately 30 h (Table S2). The parental Abs and the biAb were also detected in various muscle groups, such as the quadriceps, TA, diaphragm, and heart for up to 14 days (see Figure 3B, showing diaphragm and quadriceps as representative examples), indicating that the tissue half-life of the biAb was longer than that in the blood. This suggested that, after the Abs reached the muscle tissues and bound their targets (laminin-211 in the basal lamina and βDG on the sarcolemma, or both in the case of the biAb), the Abs persisted for a sustained period. In contrast, Abs were barely detectable in non-target tissues. There was little to no signal in the liver or spleen on day 4, the earliest collection time (Figure 3C), suggesting that the longer half-life of the Abs in the muscle was due to binding to their respective cellular targets.

As a proof of concept, LARGE^myd-3J homozygous mice were injected with the biAb into the tibialis anterior (TA) muscle; the left TA muscles were injected with the biAb on days 1 and 4, while the right TA muscles were injected with the parental Abs as controls. On day 5, Evans blue dye (EBD) was injected intraperitoneally into the mice, and the animals were then subjected to a forced treadmill exercise to induce muscle damage. As shown in Figures 2C and 2D, the EBD-positive fiber counts in the biAb-treated TA muscles were significantly (~50%) less than those in the control-treated TA muscles, suggesting that treatment with the biAb conferred a measure of protection against exercise-induced damage. We interpret that this was due to biAb-mediated reconnection of laminin-211 to βDG. We also confirmed that administering a mixture of the parental Abs to either laminin-211 or βDG did not exhibit a dominant-negative effect by conducting the same experiment in wild-type mice (Figure 2C).

Systemically Delivered Abs Are Localized in the Muscle Sarcolemma

With protein replacement therapies, biotherapeutics are typically administered to patients via intravenous infusions. Hence, for this concept to be efficacious in patients with α-dystroglycanopathy, systemic delivery of the biAb needs to result in localization of the agent in a majority of muscle tissues, particularly the sarcolemma, and the biAb needs to be sufficiently stable *in situ*. To evaluate this, mice were injected via the tail vein with either the biAb or a mixture of the two parental Abs (as a control), and the concentration of the Abs in the blood, muscle, and non-target tissues was then measured over 14 days. Blood samples were collected after 3 h and on days 1, 2, 3, 5, 7, and 14 post-injection for assessment. Target muscle tissues (quadriceps, TA, diaphragm, and heart) as well as non-disease-relevant tissues (lung, liver, kidney, and spleen) were also collected on days 4, 7, and 14 post-injection (following perfu-

Systemic Delivery of the biAb Targeting Laminin-211 and βDG into LARGE^myd-3J Mice Improves Muscle Function and Confers Protection from Exercise-Induced Damage

Next, we assessed whether systemic delivery of the biAb targeting laminin-211 and βDG protected the muscles of the LARGE^myd-3J mice from exercise-induced damage and, more importantly, improved their function. As the homozygous LARGE^myd-3J mice (9–13 weeks) presented with phenotypic variability, several parameters comprising age, hindleg splay score, grip strength, wire-hang time, baseline serum creatine kinase (CK) level without treadmill exercise, and CK level after forced treadmill exercise (Figures S3A–S3F) were used to randomize the mice into treatment groups with similar parameters. After randomization, groups of LARGE^myd-3J mice were treated with the biAb or a mixture of the parental Abs or saline as controls. Wild-type mice were also administered the biAb to assess the effect of the biAb on normal muscle function.

Following biAb treatment, LARGE^myd-3J mice showed a noticeable improvement in grip strength starting at 2–3 weeks (Figure 4A), and this improvement continued until ~5 weeks post-treatment,
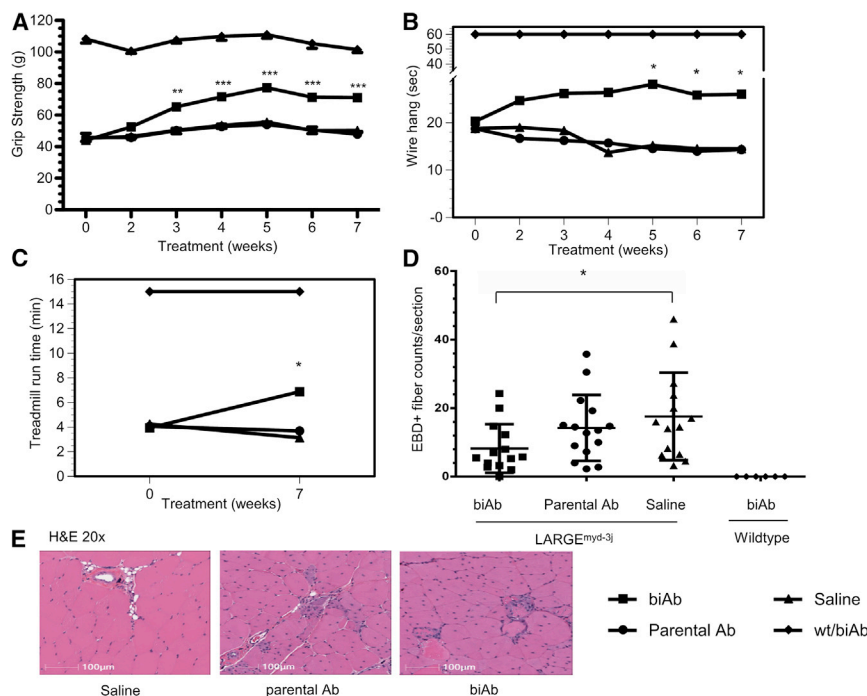
Figure 4. Systemic Delivery of biAb Improved Muscle Function in LARGE^{myd-3J} Mice and Protected Muscles from Exercise-Induced Damage

(A) Grip strength of mice over time. Mice treated with the biAb showed significantly greater grip strength than those administered the parental Abs starting at 2–3 weeks post-treatment. This improvement reached a plateau at ~4–5 weeks post-treatment. (B) Wire-hang times of mice measured over time after treatment; 60 s was used as the cutoff. (C) Treadmill run time measured over time after treatment, with 15 min as the cutoff. (D) EBD-positive fiber counts in TA muscles of LARGE^{myd-3J} mice after forced treadmill exercise. Mice treated with the biAb showed significantly fewer EBD-positive fibers in the TA muscle than saline-treated control mice, indicating a protective function of the biAb. However, compared with mice administered the parental Abs, biAb-treated mice only showed a trend toward improvement. No EBD-positive fibers were detected in the muscles of wild-type mice. (E) Representative H&E-stained sections of quadricep showed no significant histopathological changes with parental or biAb treatment. Statistical analysis was performed using one-way ANOVA followed by Tukey's test. The data are indicated as the mean ± SEM. Significance is compared to parental controls unless otherwise indicated. *p < 0.05, **p < 0.01, and ***p < 0.005. n = 16 per group.

when it appeared to reach a plateau. biAb-treated LARGE^{myd-3J} mice (at the end of the study) attained nearly 70% of the grip strength noted in the wild-type mice, compared to the parental Ab- or saline-treated control mice that maintained ~55% of the grip strength noted in wild-type mice. In the wire-hang test (Figure 4B), a trend toward improvement was noted in the LARGE^{myd-3J} mice after 2–3 weeks of treatment with the biAb, with a significant change attained after 5 weeks. The magnitude of the improvement in the wire-hang test was not as large as that in the grip strength test. Statistical significance was attained due, in part, to the continual decline in the performance of the control LARGE^{myd-3J} mice. There was no significant difference in body weight between groups (Figure S4A).

The mice were subjected to the forced treadmill exercises only at the start (baseline) and the end (7 weeks of treatment) of the study to minimize muscle damage and fatigue that might have confounded the results of the other behavioral tests. As shown in Figure 4C, the untreated LARGE^{myd-3J} mice were only able to run for ~4 min at the start of the study, and endurance decreased further over time. In contrast, the animals treated with the biAb showed an improved run time of ~8 min at the end of the study, which represented a 2-fold increase over that noted for the control mice. We attribute these improvements in both the behavioral and muscle function tests to biAb-mediated re-engagement of laminin-211 with βDG. To assess whether treatment with the biAb also conferred some measure of protection against exercise-induced damage, we used the EBD assay. As shown in Figure 4D, the biAb-treated LARGE^{myd-3J} mice exhibited significantly lower numbers of EBD-positive fibers in the TA muscle, suggesting that the biAb provided some protection against exercise-

induced muscle damage. However, the number of EBD-positive fiber counts in other muscle types, such as the force-bearing quads, did not show an improvement with treatment (data not shown). It is possible that, with these force-bearing muscles, excessive running on the treadmill may have induced additional muscle damage in the treated animals. We also observed no improvement in CK levels (Figure S4B), which could also be explained by this excessive running. Consistent with this premise is the finding that the histopathological changes in the quads of biAb-treated and control-treated mice were not significantly different (Figure 4E). It is also possible that the lack of improvement in the quads was due to the relatively short duration of treatment that resulted in the delivery of suboptimal concentrations of the biAb to these muscles. It should also be noted that the LARGE^{myd-3j} mice exhibited only modest histopathological changes between 5 and 10 months of age that hampered observations of small improvements (Figure S3J). This lack of histopathological changes could be specific to the LARGE^{myd-3j} model.

Unlike the physiological binding of laminin-211 to αDG O-linked matriglycans, which is multivalent,[29] that of the biAb between laminin-211 and βDG is monovalent. Moreover, the binding avidity of laminin-211 to the matriglycans (~6 nM) is significantly higher than that of biAb to laminin-211, which, we determined, is at ~30 nM (Table S1).[16] Thus, the overall binding of laminin-211 to dystroglycan mediated by the biAb was anticipated to be much weaker than under normal physiological conditions. In addition, it is not known whether binding of laminin-211 to the integrins, proteoglycans (heparin), or glycolipids (sulfatides) may also contribute to protecting the muscle membrane from exercise-induced damage.
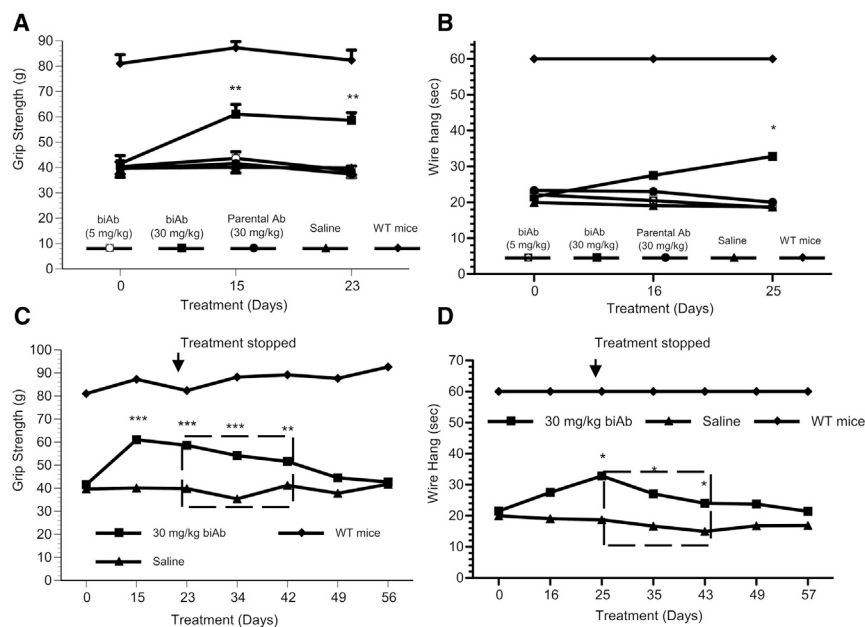
Figure 5. Dose-Response Study and Measurement of Duration of Efficacy

(A) Improvement in the grip strength of LARGE[myd-3j] mice following biAb-2 treatment for 3 weeks. (B) Improvement in the wire-hang time of mice following biAb-2 treatment for 3 weeks. Muscle function improved over the first 3 weeks with biAb-2 treatment, as observed in Figure 4A. (C and D) Grip strength (C) and wire-hang (D) performances were monitored for 5 weeks after treatment was stopped (at 3 weeks). The boxed area indicates that, during the first 2 weeks after cessation of treatment, the muscle function improvement remained significant, but it slowly returned to the baseline level by 5 weeks. Statistical analysis was performed using one-way ANOVA followed by Tukey's test. The data are indicated as the mean ± SEM. Significance is compared to parental controls; *p < 0.05, **p < 0.01, and ***p < 0.005. n = 12 per group. Boxed area indicates sustained benefits to muscle function after treatment cessation.

These differences may limit the translatability of this strategy to patients. While a biAb-mediated therapy may improve muscle function (patients attain greater physical strength), because it does not confer protection from exercise-induced muscle damage, the benefit may be modest and short-lived.

To address some of the aforementioned limitations, we generated a biAb in a different format (e.g., CODVIg) that limits the confounding issue of steric hindrance.[27] Unfortunately, the CODVIg construct was limited by production issues and could not be made in quantities to support *in vivo* testing. Thus, we also evaluated the Duobody format[29] and were successful in generating amounts of the biAb to support testing in animals.

Efficacy of Duobody biAb Is Dose Dependent and Is Sustained for 2 Weeks Post-treatment

The selection of the 30 mg/kg dose used in the studies described earlier was based on pilot studies showing evidence of efficacy at this dose (data not shown). As the biAb (in TBTI format) used in these studies demonstrated lower affinity (due to steric hindrance) to laminin-211 than the parental Ab (Figure S2B, left panel), we elected to engineer an improved version based on the Duobody format[29,30] (biAb-2) with higher affinities to both laminin-211 and βDG. This biAb-2 was used in a separate dose-response study in LARGE[myd-3J] mice. We tested two doses: 5 mg/kg (which was anticipated to be ineffective based on earlier pilot studies) and 30 mg/kg. As shown in Figures 5A and 5B, the mice administered 30 mg/kg of biAb-2 demonstrated improved muscle function at 3 weeks post-treatment, while those treated with 5 mg/kg showed no change when compared to the control mice that were administered saline or the parental Ab. No significant difference in body weight was observed between the groups (Figure S4C).

Since the biAb was detected in tissue for more than 14 days (Figure 3B), the longevity of the noted efficacy was also evaluated. Mice were treated with 30 mg/kg of biAb-2 for 3 weeks, and their performance was followed for an additional 5 weeks without additional treatments. As shown in Figures 5C and 5D, the biAb-2-treated animals demonstrated slow, progressive declines in grip strength and wire-hang time following treatment cessation; however, statistically significant improvements were maintained (in both tests) for 2 weeks after treatment cessation. CK levels appeared to decrease with 30 mg/kg of biAb treatment; however, this positive trend was not statistically significant (Figure S4D). At 5 weeks after treatment cessation, the performance of the biAb-2-treated mice had returned to the baseline values noted before the start of the treatment.

It has been shown that AAV9-mediated expression of LARGE1 (under the transcriptional control of a muscle-specific promoter) is efficacious at correcting the aberrant O-glycosylation on αDG and ameliorating the muscle pathology in LARGE-deficient mice.[31] We have independently confirmed these observations using a similar AAV vector. In Figure S5A, we show that glycosylation was restored above wild-type levels with AAV treatment. Using the extensor digitorum longus (EDL) muscle eccentric contraction damage assay, we further demonstrated that the EDL muscles of AAV9-LARGE1-treated mice were fully protected from eccentric contraction-induced damage, a finding that we did not observe with the biAb-2 in short-term studies. Thus, a longer term study (10 weeks of treatment) with biAb-2 was performed to determine whether accumulation of higher amounts of biAb in EDL may confer greater protection. As anticipated, an improvement in grip strength was noted that was sustained over the entire treatment period (Figure 6A); however, the magnitude of improvement was less than that seen in animals administered AAV9-LARGE1. At the end of the study, a subset of mice treated with AAV9-LARGE1, biAb-2, or the parental-Ab-treated mice were subjected to the EDL assay. As shown in Figure 6B, 4 of
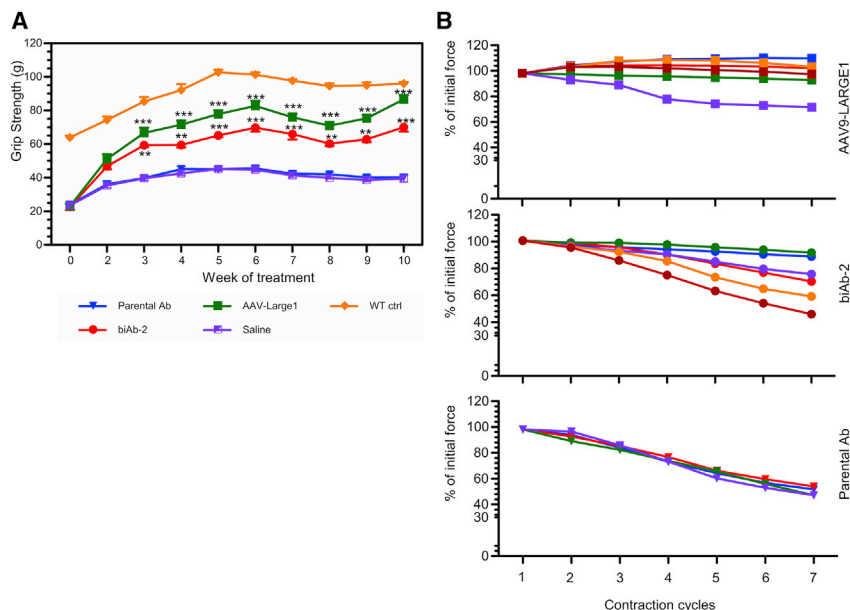
Figure 6. Long-Term Study Comparing the Efficacy of Mice Treated with AAV9-LARGE1 or biAb-2

(A) Improvements in the grip strength of LARGE^{myd-3j} mice following treatments with parental Ab (blue triangles), saline (purple half-filled squares), AAV9-LARGE1 (green squares), and biAb-2 (red circles) for 10 weeks; wild-type mice were used as control (orange diamonds). In this study, treatment was initiated in younger LARGE^{myd-3j} mice at ~6 weeks of age, and grip strength was lower at the beginning of the study (~20 g) due to younger age, since the mice were smaller. These values increased with age so that, at 9 weeks, they were at ~40 g in the control-treated LARGE^{myd-3} mice. Improvements in strength were evident in the AAV9-LARGE1- and biAb-2-treated cohorts. Statistical analysis was performed using one-way ANOVA followed by Tukey's test. The data are indicated as mean ± SEM. Significance is compared to parental controls; **p < 0.01 and ***p < 0.005. n = 14–16 per group. (B) Eccentric contraction-induced damage assay of EDL muscles of LARGE^{myd-3j} mice treated with AAV9-LARGE1 (squares), biAb-2 (circles), and parental Ab (triangles). For each symbol, different colors indicate different individual animals. AAV9-LARGE1 treatment achieved near-complete protection, whereas biAb-2 treatment only managed partial protection in most of the animals, with a lesser degree than that with AAV9-LARGE1. Treatment with the parental Ab did not offer measurable protection.

the 6 EDLs from biAb-2 treated mice showed improved protection (albeit to differing extents), compared to none in the parental-Ab-treated mice. As expected, full protection of EDL muscles was observed in all the AAV9-LARGE1-treated animals. Prior to the contraction assay, we observed no change in twitch or tetanic force in the biAb-treated animals compared to the parental-Ab-treated mice (Figures S5B and S5C). This result is consistent with the results from the EBD-positive fiber assay and suggests that improving the affinity of the biAb and increasing the duration of treatment with the biAb may confer greater protection from exercise-induced muscle damage. Histopathological analysis demonstrated that significant improvement was attained with AAV9-LARGE1 treatment, but no noticeable change was observed with biAb-2 treatment (data not shown). This seems to be contradictory to the results of the EDL assay in which muscle damage protection was attained in some of the animals, albeit to a lesser degree, compared to AAV9-LARGE1. We speculate that this could be due to a combination of factors, including the time needed for biAb accumulation in muscles to a critical threshold concentration necessary to effectively and robustly protect the muscle; the time required for muscle repair to complete under normal conditions is estimated to be ~3 weeks. By contrast, the onset of LARGE1 expression from AAV9-LARGE1 occurred rapidly (within a few days) and was, therefore, able to more rapidly restore the matriglycan on αDG to confer protection from muscle damage. In addition, the ratio of biAb-mediated binding of laminin-211 to βDG was only 1:1, which is much less than that of matriglycan to laminin-211. Finally, the affinity of the biAb to its ligands was less than that with matriglycan. Thus, further improvements to the affinity and binding molar ratios (e.g., via multi-specific antibodies) could

be explored to extend our findings of improved muscle function to histopathological normalization and long-term benefits in the clinic.

DISCUSSION

Intuitively, the genetic heterogeneity of αDG-related muscular dystrophies would require a personalized approach to managing each of the 18 causative genes identified thus far. Indeed, gene augmentation therapy to reconstitute the expression of the respective gene products has demonstrated success in several murine models of this group of diseases.[31–36] However, challenges associated with developing systemic gene therapy for muscular dystrophies remain. These challenges include the relatively low efficiency of current gene delivery vectors (such as AAV vectors) in transducing the mass of affected muscles and the presence of pre-existing neutralizing Abs against the viral vectors. Both factors limit the number of eligible patients amenable to this approach. Nevertheless, innovative approaches continue to be sought to improve the tropism and efficiency of AAV vectors.[37,38] While developing a separate gene delivery vector for each of the diseases is rational, this is arguably inefficient and offers a high cost-to-benefit ratio, particularly given the low prevalence of patients associated with each subset of diseases. For this reason, we rationalized that a more generalized approach that could ameliorate several subtypes of α-dystroglycanopathies might be more advantageous. Toward this aim, we engineered biAbs that could act as a surrogate molecular linker to reconnect the generalized loss of binding between laminin-211 and αDG in the LARGE^{myd-3J} mouse model. This approach could potentially treat other subtypes of α-dystroglycanopathies; however, additional animal models need to be tested.

The preclinical data generated in the LARGE[myd-3J] mice using the biAbs that we developed suggest that the biAbs were able to engage both laminin-211 and βDG simultaneously (see Figures 4, 5, 6, and S4A for potential mechanisms of action). Only the biAbs, not the parental Abs (administered as a mixture that engaged their targets separately), conferred a beneficial outcome (Figures 4, 5, 6, S6A, and S6B), suggesting that biAbs engaged both targets concurrently. However, attempts to visualize this physical interaction by immuno-fluorescence imaging were unsuccessful due to the close proximity of the sarcolemma to the basal lamina (Figure 3B). Thus, higher resolution and more sensitive physical and biochemical approaches are likely needed to address this specifically.

Evidentiary demonstration of efficacy was noted in biAb-treated LARGE[myd-3J] mice using validated muscle function assays. The improvements were highly significant but did not reach the levels noted in healthy animals. Moreover, with some of the tests (e.g., wire-hang tests), maximal benefit was realized after 5 weeks of treatment, and performance did not improve further with additional biAb supplementation. Possible reasons for this include the generation of anti-drug Abs; indeed, low anti-biAb Ab levels were detected after 4 weeks of treatment (data not shown). Another, and perhaps more likely, possibility is the inability of the biAb (in its current configuration) to correct the defects at neuromuscular junctions (NMJs), as this requires the restoration of the linkage between agrin and dystroglycan. The inability of the biAb to fix the abnormal NMJs noted in the LARGE[myd-3J] mice (Y.Z., N.G., Z.L., and D.S.B., unpublished data) may have contributed to the confounding behavioral data. Indeed, the hindleg splay assay, which requires proper functioning of the peripheral nerves, did not improve with treatment with the biAb. Concordant with this premise, McKee et al.[39] recently reported on the ability of a chimeric protein comprising the N-terminal domain of laminin α2 subunit fused to a nidogen fragment (that binds to the laminin γ1 subunit) to repair a defect in laminin-211 polymerization in Lama2[dy-2j] mice. While the forelimb strength of the treated Lama2[dy-2j] mice was completely restored, that of the hindlegs was only minimally improved, likely due to the lack of correction of the amyelination of the hindlimb nerves. When a grip strength test was performed with all four limbs (as in our study), the maximal improvement attained was approximately 50% that of the wild-type mice, which was similar to what we observed in the LARGE[myd-3J] mice. If this explanation is true, this represents an anticipated limitation of the biAb strategy, because it will not correct the binding of DG to ligands other than laminin-211, such as agrin, neurexin, and pikachurin. biAb can correct the muscular dystrophic aspects of patients with α-dystroglycanopathies but not their neurological or ocular abnormalities. In this regard, we posit that this strategy, if successful in humans, would be most applicable for α-dystroglycanopathy patients with no or moderate CNS involvement, such as those with LGMD2I and related disorders.[2,10] However, it should be noted that the structural brain defects in patients with the most severe α-dystroglycanopathies (e.g., WWS or MEB) are incurred *in utero* and, thus, may not be amenable to postnatal correction by any means, even with AAV gene therapy. Nevertheless, an improvement in mus-

cle function in the severely affected patients with CNS involvement may still offer consequential benefits to reduce caregiver burden and extend the patients' lives.

Given the significant but incomplete correction of muscle function in this study, complementary therapies may be needed to confer a more transformative change in patients with α-dystroglycanopathies. These could include, for example, the combined use of the biAb with follistatin or anti-myostatin to enhance muscle regeneration. Hence, it may be that the biAb represents but one of a cocktail of drugs that could be used for this group of disorders. Greater improvement may also be realized if the mice are treated at an earlier age, before there is significant and perhaps irreversible damage, or with a multi-functional antibody with multi-valency binding to laminin-211 that may offer better binding and muscle damage protection. Finally, our novel strategy of using a biAb as a molecular linker to reconnect structural aberrations could be considered for related or adjacent neuromuscular diseases.

MATERIALS AND METHODS
Expression of Human and Mouse LG5 or LG4/5 Domains of Laminin α2 Subunit and βDG ECD

The LG domains of the human and murine α2 chain of laminin-211 and the ECDs of human and murine βDG were expressed in HEK cells to ensure proper folding and glycosylation. The boundaries of the LG domains were determined based on the publications of Talts et al.[40,41] The LG5 domains were codon optimized for mammalian expression and synthesized with an N-terminal AviTag and an HPC4 tag. Constructs were subcloned into a mammalian expression vector and used to transfect Expi293F cells using ExpiFectamine reagent (Thermo Fisher Scientific). After 7 days, the soluble protein was purified from the supernatant with an anti-HPC4 Ab that was amine coupled to an agarose resin. Alternatively, LG4/5 domains were codon optimized and paired with an mIgG2a Fc fusion partner and a TEV cleavage site to allow for removal of the IgG domain. After synthesis, each construct was subcloned into a mammalian expression vector and was used to transfect Expi293F cells using ExpiFectamine reagent (Thermo Fisher Scientific). After 7 days, soluble protein was purified from the supernatant with a HiTrap MabSelect SuRe column (GE Healthcare). When necessary, the fusion partner was cleaved off using TurboTEV enzyme (Nacalai USA, San Diego, CA, USA) and removed by purification using Ni-NTA resin (QIAGEN).

To express the ECD of murine βDG, an *Escherichia coli* codon-optimized cassette encoding the murine βDG ECD and a C-terminal HPC4 tag was synthesized and subcloned in frame to an N-terminal maltose binding protein (MBP) fusion partner in a Novagen pET22b vector. The vector was used to transform Origami B(DE3)pLysS cells (Novagen). Protein expression in bacteria was induced with 1 mM isopropyl β-D-1-thiogalactopyranoside. For protein purification, cell pellets were resuspended in 50 mM Tris-HCl, 150 mM NaCl (pH 7.4) containing EDTA-free protease inhibitors (Roche) and lysed by sonication. The lysate was clarified by centrifugation and filtration

and then processed on an amylose resin (New England Biolabs) equilibrated with 50 mM Tris-HCl, 150 mM NaCl (pH 7.4). The fusion protein was eluted using the same buffer containing 10 mM maltose. Calcium (final concentration, 1 mM) was added to the amylose elution, and the fusion protein was purified further on an anti-HPC4 affinity column. Alternatively, βDG ECD was codon optimized and paired with an mIgG2a Fc fusion partner and a TEV cleavage site to allow for the removal of the IgG domain as described for LG4/5 domains.

Ab Generation
Mouse Immunization
BALB/c mice were immunized with human βDG, human LG-5, or human LG-4/5 and then boosted with these proteins 3–4 times every 2 weeks. Mice immunized with human LG-4/5 were additionally boosted three times with human merosin every 2 weeks and once with a synthetic peptide with a sequence identical between human and mouse LG-5 (amino acid sequence GFAKAVGGFKV GLDLLVEFE).

Hybridoma Generation
Hybridoma cells were made by fusing mouse myeloma cells (from the BALB/c B-lymphoblast cell line SP2/0 fused with Sendai virus) deficient in adenosine phosphoribosyltransferase (APRT) with spleen cells from immunized mice. Hypoxanthine, azaserine, and thymidine (HAT) selection and serial dilutions were performed to achieve single-cell clonality.

Design of biAb Recognizing LG4/5 and βDG ECD
A biAb recognizing both LG5 and βDG was designed with one set of anti-LG5 V_L and V_H sequences and one set of anti-βDG V_L and V_H sequences in two different anti-LG5 and βDG orientations, resulting in two biAb constructs (anti-LG5 × βDG and anti-βDG × LG5) in the TBTI format (Figure 2A).[42] Briefly, the V_H sequences of a pair of binders were fused with a linker (GGGGS)$_2$ and then fused either to human IgG1 (huIGHG1; GenBank: Q569F4) or murine IgG1 (muIGHG1; GenBank: AAA75163.1) heavy-chain Fc. The V_L sequences of paired binders were fused to the constant human kappa chain (huIGKC; GenBank: Q502W4) or mouse kappa chain (muIGKC; GenBank: BAB33404). An improved biAb (biAb-2) was also created with higher affinity Abs to laminin-211 and βDG in an alternative biAb Duobody format[29] that was not subject to steric hindrance of the inner V_L and V_H.

Construction of Expression Plasmids for the Production and Purification of Recombinant mAbs and biAbs
The light-chain and heavy-chain DNA fragments of the parental mAbs and biAbs were cloned into the episomal expression vector pXL, an analog of the pTT vector described by Durocher et al.,[43] creating plasmids for transient mammalian expression of biAbs in Expi293 cells. The mAbs and biAbs from cell culture media were purified using a HiTrap MabSelect SuRe column (GE Healthcare) following the manufacturer's protocol, eluted with 0.1 M citrate (pH 3.0), and neutralized immediately with 1 M Tris-HCl (pH 8.0).

The mAbs and biAbs were buffer exchanged into PBS, filter sterilized (Millex-GV 0.22-μm syringe filter, SLGV033RS), and used for *in vitro* characterization and *in vivo* applications.

Dot Blot, SPR, and ELISA Characterizations of mAbs and biAbs
Dot Blot.   Various antigens (BioLamina) used for dot blotting were serially diluted in PBS at 5× per dilution, typically with the highest amount at 50 ng total protein and the lowest at 0.08 ng. Five microliters of each sample was placed onto a nitrocellulose membrane (Bio-Rad) with heavy filter paper using a 20-μL multichannel pipette. After the membranes were air dried for 15 min, the membranes were processed as in a regular western blot. Membranes were blocked by incubation with 5% (w/v) non-fat milk (Bio-Rad) in Tris-buffered saline (TBS) with 0.05% Tween-20 (TBS-T) for 1 h at room temperature, and then primary Abs (typically at 1 μg/ml) in 5% low-fat milk were added to the membrane and mixed gently for an additional 1 h at room temperature. Membranes were washed three times in TBS-T for 5 min each. Goat anti-mouse IgG-HRP (horseradish peroxidase) (Pierce, 1:5,000 dilution) or goat anti-human IgG-HRP (Millipore, 1:5,000 dilution) in 5% milk was added and incubated with membranes for another 1 h, followed by three washes in TBS-T as described earlier. Blots were developed with SuperSignal Chemiluminescent Substrate (Pierce) for 5 min and exposed to film for various amounts of time ranging from 1 s to 10 min.

ELISA.   A sandwich ELISA was developed by taking advantage of the difference in Ab binding between mouse and human IgG Fc (Figure S2C). First, 96-well plates were coated with 100 μL (0.5 μg/mL) LG5 in PBS overnight at 4°C, after which the coating solutions were removed. The plates were then blocked with 5% fetal bovine serum in PBS for 1 h, followed by three washes with PBS. A 100-μL aliquot of biAb (or a single parental Ab to laminin-211 or βDG) with the human IgG backbone (anti-laminin α2 × βDG) at 10 μg/ mL was added to each well and incubated at room temperature for 2 h with gentle shaking. Thereafter, the plates were washed three times with PBS, and various concentrations of βDG ECD fused to mouse Fc (βDG ECD-mFc) in 100-μL aliquots were added to the wells in 2-fold serial dilutions, followed by incubation for 2 h with gentle shaking at room temperature. After three washes with PBS, HRP-conjugated anti-murine Fc secondary Ab was added and incubated for 45 min. The plates were washed four times with PBS and developed for colorimetric measurements. Signals could be detected only when both LG5 and βDG ECD-mFc were added in the assay. No signal was detected when βDG ECD-mFc was omitted or when only one parental Ab was added. This procedure could be reversed using βDG for coating followed by LG5-mFc with similar results (data not shown).

SPR Analysis of Abs.   A Biacore T100 kinetics/affinity assay was optimized to capture the Abs (mAbs and biAbs) on chips and screen for ligand-binding affinities. Briefly, a Biacore human or mouse Ab capture kit (GE Healthcare) was used to immobilize ~10,000 RU of mouse anti-hIgG or rabbit anti-mIgG on a CM5 Series S biosensor using amine-coupling techniques. Abs and a negative isotype control

were diluted to 20 μg/mL in HBS-EP+ running buffer (10 mM HEPES, 150 mM NaCl, 3 mM EDTA, 0.005% polysorbate 20). The Abs were captured for 60 s at 10 μL/min, and human and murine LG5 or LG4/5 or human βDG and MBP-mβDG ECD fusion proteins were diluted to 80, 40, 20, 10, 5, 2.5, 1.25, and 0 nM in HBS-EP+ running buffer. Analytes were injected for 5 min to measure association, followed by 10 min of buffer for dissociation at 30 μL/min. The Ab capture surface was regenerated between cycles using a 60-s injection of 12 mM HCl at 30 μL/min. Reference-subtracted sensorgrams were fitted to a 1:1 binding model using Biacore T100 Evaluation software v.2.0.2. The process of sequential binding of LG5 and βDG to Abs on Biacore was essentially the same as described earlier, except that a 100-nM solution of one analyte was injected for 2 min at 30 μL/min, immediately followed by injection of the second analyte, also at 100 nM, to detect the second binding event (Figure S2B).

Animals

The LARGE$^{myd-3J/GrsrJ}$ mice (stock #008581) were purchased from the Jackson Laboratory after custom cryo-recovery and breeding between heterozygous males and females. A genotyping method was developed for the myd-3j mutation (Y.Z., N.G., and Z.L., unpublished data). Homozygous mice were confirmed by phenotypic screenings, and both male and female mice were used for the studies in this paper. Homozygous mice generally began to exhibit symptoms as early as weaning. They initially displayed an inability to splay their hindlegs outward when held up by the tail, progressing to a swaying gait and subsequently dragging of their hindlegs. Homozygous LARGE^{myd-3J} mice were also confirmed biochemically by the absence of O-linked IIH6-positive glycans and the lack of laminin-211 binding in a laminin-overlay assay. A detailed characterization and validation of this model will be published separately. Animal experiments were conducted in accordance with the guidelines issued by the U.S. Department of Health and Human Services (NIH Publication no. 86-23) and were approved by Sanofi Genzyme's Institutional Animal Care and Use Committee (IACUC).

Biodistribution of mAbs and biAb in Mice

Wild-type mice at ∼8 weeks of age were injected intravenously (i.v.) via the tail vein with 30 mg/kg of the biAb or a mixture of parental Abs (15 mg/kg each) with the mIgG1 backbone. Blood serum samples were collected by submandibular vein bleeding at 3 h; 24 h; and 2, 3, 4, 7, and 14 days after administration. The parental Ab or biAb level at each time point was measured using an ELISA developed in house. Briefly, a 96-well plate was coated with 100 μL per well of mouse MBP-βDG at 0.5 μg/mL overnight at 4°C. The plate was washed with PBS and blocked with blocking buffer containing 5% BSA for 1 h followed by 3 washes with PBS; and 100 μL of each serum sample at various dilutions was then added into the wells. The plates were incubated for 2 h with gentle shaking at room temperature and washed 4 times with PBS. HRP-conjugated goat anti-mouse IgG was added and incubated for 45 min. After 6 washes with PBS, the plate was developed and measured via colorimetry. Purified biAb solutions in assay diluent at various concentrations were used as standards. Blood half-life of antibodies was estimated according to the graph in Figure 3A.

To determine tissue biodistribution, four mice per group were perfused and sacrificed at days 4, 7, and 14. Various muscle tissues and non-target tissues were harvested in optimum cutting temperature (OCT) compound (EM Bioscience), snap-frozen in isobutane/dry ice, and stored at −80°C until use. To stain for the mAbs and biAb in tissues, tissues were cryo-sectioned at 10-μm thickness, air-dried unfixed, and stained with fluorescently labeled anti-mIgG Fc Ab.

Local Injection of biAb into the TA Muscle of the LARGE^{myd-3J} Mice and Analysis of Muscle Damage

A group of LARGE^{myd-3J} mice (n = 10) were given intramuscular injections into the left and right TA muscles. The left TA muscle received two injections of biAb-mIgG1 (at 0.7 μg/μL in 50 μL saline per injection with 29G needles) 3 days apart. The right TA muscle received two injections of 50 μL parental Ab mixture per injection. One day after the last intramuscular injection, all the mice received intraperitoneal injections of EBD (at 10 mg/mL, with 50 μL given per 10 g body weight). Eighteen hours after intraperitoneal injection of EBD, all the mice were forced to exercise on a treadmill (Columbus Instruments) until exhaustion. After euthanasia and perfusion, the TA muscles were removed, cut, and placed in OCT. The tissue was cryo-sectioned at a thickness of 10 μm at four different levels in triplicate, 100 μm apart. For staining, the slide sections were quickly dipped into cold PBS and fixed in ice-cold acetone for 15 min. Slides were washed (3 × 5 min) in PBS, outlined with a hydrophobic marker, and blocked with 2% BSA with 1:100-diluted normal goat serum in PBS overnight at 4°C. The next day, the slides were incubated with anti-mouse IgG Alexa Fluor 488 (Invitrogen) at 1:400 dilution for 2 h at room temperature. Slides were washed 3 times (5 min each) with TBS-T and then washed 1 time for 5 min with PBS and mounted with VectaShield mounting medium with DAPI. Slides were sealed with coverslips and visualized with an inverted microscope (Olympus IX71) using appropriate filter sets. Pictures were acquired using a charge-coupled device (CCD) Hamamatsu digital camera (C8484) and MetaMorph software (v.7.8.1.0). Each field was exposed for 1 s for Alexa Fluor 488 and EBD or 0.5 s for DAPI. The pictures were subsequently overlaid using Adobe Photoshop CS5.

For EBD-positive fiber counting, tissue sections were processed as described earlier. The EBD-positive fibers in each section were counted manually twice at each of the four levels for both the left and right TA muscles of each animal. The numbers of EBD-positive fibers in the sections at four levels were averaged to yield the EBD-positive fibers per TA muscle sample. In every animal analyzed, there were fewer EBD-positive fibers in the biAb-injected left limb than in the parental Ab-injected right limb. The difference between the left and right TA muscles reached statistical significance (p < 0.05) as determined by a paired Student's t test.

Method for IP

For each sample, 90 mg frozen muscle tissue that was locally injected with saline, parental Ab, or bispecific antibody as described earlier was placed into a 2-mL bead beater tube together with 1.8 mL ice-cold immunoprecipitation (IP) lysis buffer (TBS [pH 8], 1% NP40,

0.5% sodium deoxycholate, 10 mM EDTA, 10 mM EGTA, PMSF, and protease inhibitors) and one sterile 5-mm steel bead. The samples were subjected to 2 cycles (10 min per cycle) in the bead beater (TissueLyser II, QIAGEN) at maximum speed (30Hz) at 4°C, after which the samples were removed and then slowly rotated for an additional hour at 4°C. Samples were then centrifuged at 13,000 rpm for 10 min at 4°C, and the supernatants were removed and aliquoted (∼900 μL). For direct IP of DGC, an anti-βDG antibody (Leica clone 43DAG1/8D5), which has a different epitope than that in our biAb treatment, was utilized. For *in vivo* bound IP, no additional antibody was added. The supernatant generated as described earlier was incubated overnight via slow rotation at 4°C. Protein A/G bead slurry was then added and further incubated overnight via slow rotation at 4°C. The resulting mixture was centrifuged (2,000 rpm for 5 min), and the supernatant was removed. The resulting pellet was washed extensively with TBS, re-suspended in 120 μL SDS-PAGE loading buffer with fresh β-mercaptoethanol, boiled for 10 min, and centrifuged (5,000 rpm for 5 min). The supernatant was assessed by western blot using the polyclonal AF6868 DAG1 antibody (R&D Systems).

Systemic Delivery of biAb into LARGE^{myd-3J} Mice and Analysis of Muscle Function Improvement and Damage Protection

To ensure that the LARGE^{myd-3J} mice (between 9 and 13 weeks of age) started with a similar performance baseline prior to testing, several parameters were measured, including hindleg splay, grip strength, wire-hang time, and treadmill run time as well as CK levels (Figure 4). Based on these test results, the LARGE^{myd-3J} mice were randomized into three groups (n = 16) with similar average scores. One group received the biAb (30 mg/kg), and the other two groups received the parental Abs (a mixture of anti-laminin-211 at 15 mg/kg and anti- βDG at 15 mg/kg) or saline as a control. As an additional control, another group of wild-type mice (n = 6) received the same dose of biAb. The mice were dosed i.v. via tail vein injection twice a week for a total of 7 weeks. One day after the last injection, all the mice were tested for wire-hang time, grip strength, and hindleg splay, after which they received EBD as described earlier. After waiting overnight, all the mice were exercised via a forced treadmill run until exhaustion (with 15 min as the cutoff). One hour after treadmill running, the animals were euthanized with CO_2 and perfused with PBS, and various muscles were collected and placed in OCT compound. The muscles were cryo-sectioned and processed for EBD-positive fiber counting as described earlier. Statistical analysis was performed with one-way ANOVA followed by Tukey's multiple comparison test. A similar study with older mice (between 19 and 22 weeks of age) was repeated for confirmation, with two groups of LARGE^{myd-3J} mice receiving the biAb or saline and a wild-type group receiving saline. For the treatment withdrawal study, mice were dosed with 5 or 30 mg/kg of the biAb, parental Abs, or saline for 3 weeks, when a significant improvement on grip strength and wire-hang time was observed. Then, treatment was stopped, but behavioral tests were continued weekly for the 30 mg/kg biAb group, the saline control group, and the wild-type group until they reached baseline or control levels. The 5 mg/kg and parental Ab groups were sacrificed for tissue collection immediately after 3 weeks of treatment.

Behavioral Tests

For the hindleg splay test, the mice were lifted by their tails, and the positions of the hindlegs relative to the body were recorded and graded. The wire-hang test was conducted by placing mice on a wire grid and letting them acclimate for 1 min; then the wire grid with the mouse grasping on was slowly turned upside down in 2 s, and the time the mouse held onto the grid was recorded, with a cutoff time of 60 s. The test was repeated 3 times for each mouse, and the results were averaged. Grip strength was evaluated by placing the mice on a grip strength meter (Columbus Instruments), allowing the mouse to grasp the metal grid firmly and pulling the tail horizontally until the mouse let go; then, the force was recorded. The test was repeated 5 times, with a 1-min rest between trials. The highest and lowest readings for each mouse were removed, and the results presented are the average of the three remaining readings. For treadmill run time, mice were placed onto individual lanes of a treadmill equipped with an electric shocking grid (model 1055-SRM Exer-3/6, Columbus Instruments). The animals were acclimated to the treadmill for 5 min, and then the mice were tested with a defined protocol with increasing speed. When a mouse spent more than 3 s on the shocking grid without being able to run, the shocking grid was turned off, and the total run time was recorded. All behavioral tests were performed by researchers blinded to mouse identity and treatment, with the results revealed after testing.

Ex Vivo *EDL Force Measurement*

Contractile properties of EDL muscles isolated from wild-type and LARGE^{myd-3j} mice were measured by using a 300B dual-mode servomotor transducer and DMC/DMA software (Aurora Scientific), as described elsewhere.[44] Briefly, the distal tendon of the EDL was tied to the servomotor by using a 6-0 silk suture, and the proximal tendon was clamped to a fixed post. The EDL muscles were immediately immersed in an oxygenated bath (95% O_2, 5% CO_2) that contained modified Krebs-Ringer buffer at 25°C. Muscle length and the current of stimulation were adjusted until an isometric twitch contraction achieved the maximum force (induced by a single stimulus with a pulse duration of 0.2 ms). After the optimization, maximum twitch forces were obtained by a single stimulus with a pulse width of 0.5 ms. At the optimized muscle length (Lo), maximum isometric tetanic forces were determined by applying tetanic stimulation for 500 ms at a frequency of 120 Hz with a pulse width of 0.5 ms. The EDL muscles were subjected to 7 cycles of eccentric contraction injury by applying tetanic stimulation for 500 ms at a frequency of 120 Hz with a pulse width of 0.5 ms while the muscle was lengthened by 7.5% Lo at 0.5Lo/s during the last 200 ms. The muscles were rested for 2 min between successive contractions. Maximum tetanic force produced before the lengthening contraction was obtained at each cycle to calculate the force drop as a percentage of the force obtained during the first cycle.

Data Availability

The datasets generated during and/or analyzed during the present study are not publicly available per Sanofi intellectual property policy

but are available from the corresponding author on reasonable request pending Sanofi legal approval.

AUTHOR CONTRIBUTIONS
Y.Z. conceived the therapeutic strategy, designed the experiments, and interpreted and analyzed the data. N.G., L.M.S., H.Z. and Z.L. designed and performed the experiments and interpreted and analyzed the data. M.L. and E.B. performed experiments. B.M. and M.M. generated the hybridoma clones. E.R., C.B., C.L., L.M.S., and Y.Z. designed the biAb. E.M., J.E.S., L.M.S., and T.T. expressed, purified, and characterized the biAb. T.Y.-M. and W.F. performed the EDL assay. D.S.B. performed and interpreted histological data. Y.Z., Y.C., D.R., H.Q., W.H.B., and S.H.C. supervised the work. Y.Z. wrote the manuscript, and N.G., W.H.B., S.H.C., and L.M.S. edited the manuscript.

CONFLICTS OF INTEREST
All the authors of this paper are present or past employees of Sanofi.

REFERENCES
1. Barresi, R., and Campbell, K.P. (2006). Dystroglycan: from biosynthesis to pathogenesis of human disease. J. Cell Sci. 119, 199–207.

2. Godfrey, C., Clement, E., Abbs, S., and Muntoni, F. (2011). Exclusion of WWP1 mutations in a cohort of dystroglycanopathy patients. Muscle Nerve 44, 388–392.

3. Taniguchi-Ikeda, M., Morioka, I., Iijima, K., and Toda, T. (2016). Mechanistic aspects of the formation of α-dystroglycan and therapeutic research for the treatment of α-dystroglycanopathy: a review. Mol. Aspects Med. 51, 115–124.

4. Endo, T. (2015). Glycobiology of α-dystroglycan and muscular dystrophy. J. Biochem. 157, 1–12.

5. Toda, T. (2005). [Alpha-dystroglycanopathy (FCMD, MEB, etc): abnormal glycosylation and muscular dystrophy]. Rinsho Shinkeigaku 45, 932–934.

6. Toda, T., Kobayashi, K., Takeda, S., Sasaki, J., Kurahashi, H., Kano, H., Tachikawa, M., Wang, F., Nagai, Y., Taniguchi, K., et al. (2003). Fukuyama-type congenital muscular dystrophy (FCMD) and alpha-dystroglycanopathy. Congenit. Anom. (Kyoto) 43, 97–104.

7. Stensland, E., Lindal, S., Jonsrud, C., Torbergsen, T., Bindoff, L.A., Rasmussen, M., Dahl, A., Thyssen, F., and Nilssen, Ø. (2011). Prevalence, mutation spectrum and phenotypic variability in Norwegian patients with limb girdle muscular dystrophy 2I. Neuromuscul. Disord. 21, 41–46.

8. Poppe, M., Cree, L., Bourke, J., Eagle, M., Anderson, L.V., Birchall, D., Brockington, M., Buddles, M., Busby, M., Muntoni, F., et al. (2003). The phenotype of limb-girdle muscular dystrophy type 2I. Neurology 60, 1246–1251.

9. Brockington, M., Yuva, Y., Prandini, P., Brown, S.C., Torelli, S., Benson, M.A., Herrmann, R., Anderson, L.V., Bashir, R., Burgunder, J.M., et al. (2001). Mutations in the fukutin-related protein gene (FKRP) identify limb girdle muscular dystrophy 2I as a milder allelic variant of congenital muscular dystrophy MDC1C. Hum. Mol. Genet. 10, 2851–2859.

10. Godfrey, C., Clement, E., Mein, R., Brockington, M., Smith, J., Talim, B., Straub, V., Robb, S., Quinlivan, R., Feng, L., et al. (2007). Refining genotype phenotype correlations in muscular dystrophies with defective glycosylation of dystroglycan. Brain 130, 2725–2735.

11. Henry, M.D., and Campbell, K.P. (1999). Dystroglycan inside and out. Curr. Opin. Cell Biol. 11, 602–607.

12. Matsumura, K., and Campbell, K.P. (1994). Dystrophin-glycoprotein complex: its role in the molecular pathogenesis of muscular dystrophies. Muscle Nerve 17, 2–15.

13. Ervasti, J.M., and Campbell, K.P. (1993). A role for the dystrophin-glycoprotein complex as a transmembrane linker between laminin and actin. J. Cell Biol. 122, 809–823.

14. Stalnaker, S.H., Aoki, K., Lim, J.M., Porterfield, M., Liu, M., Satz, J.S., Buskirk, S., Xiong, Y., Zhang, P., Campbell, K.P., et al. (2011). Glycomic analyses of mouse models of congenital muscular dystrophy. J. Biol. Chem. 286, 21180–21190.

15. Inamori, K., Yoshida-Moriguchi, T., Hara, Y., Anderson, M.E., Yu, L., and Campbell, K.P. (2012). Dystroglycan function requires xylosyl- and glucuronyltransferase activities of LARGE. Science 335, 93–96.

16. Briggs, D.C., Yoshida-Moriguchi, T., Zheng, T., Venzke, D., Anderson, M.E., Strazzulli, A., Moracci, M., Yu, L., Hohenester, E., and Campbell, K.P. (2016). Structural basis of laminin binding to the LARGE glycans on dystroglycan. Nat. Chem. Biol. 12, 810–814.

17. Han, R., Kanagawa, M., Yoshida-Moriguchi, T., Rader, E.P., Ng, R.A., Michele, D.E., Muirhead, D.E., Kunz, S., Moore, S.A., Iannaccone, S.T., et al. (2009). Basal lamina strengthens cell membrane integrity via the laminin G domain-binding motif of alpha-dystroglycan. Proc. Natl. Acad. Sci. USA 106, 12573–12579.

18. Bowe, M.A., Mendis, D.B., and Fallon, J.R. (2000). The small leucine-rich repeat proteoglycan biglycan binds to alpha-dystroglycan and is upregulated in dystrophic muscle. J. Cell Biol. 148, 801–810.

19. Watanabe, N., Sasaoka, T., Noguchi, S., Nishino, I., and Tanaka, T. (2007). Cys669-Cys713 disulfide bridge formation is a key to dystroglycan cleavage and subunit association. Genes Cells 12, 75–88.

20. Groh, S., Zong, H., Goddeeris, M.M., Lebakken, C.S., Venzke, D., Pessin, J.E., and Campbell, K.P. (2009). Sarcoglycan complex: implications for metabolic defects in muscular dystrophies. J. Biol. Chem. 284, 19178–19182.

21. Koenig, M., Hoffman, E.P., Bertelson, C.J., Monaco, A.P., Feener, C., and Kunkel, L.M. (1987). Complete cloning of the Duchenne muscular dystrophy (DMD) cDNA and preliminary genomic organization of the DMD gene in normal and affected individuals. Cell 50, 509–517.

22. Sandonà, D., and Betto, R. (2009). Sarcoglycanopathies: molecular pathogenesis and therapeutic prospects. Expert Rev. Mol. Med. 11, e28.

23. Schéele, S., Nyström, A., Durbeej, M., Talts, J.F., Ekblom, M., and Ekblom, P. (2007). Laminin isoforms in development and disease. J. Mol. Med. (Berl.) 85, 825–836.

24. Holmberg, J., and Durbeej, M. (2013). Laminin-211 in skeletal muscle function. Cell Adhes. Migr. 7, 111–121.

25. Tisi, D., Talts, J.F., Timpl, R., and Hohenester, E. (2000). Structure of the C-terminal laminin G-like domain pair of the laminin alpha2 chain harbouring binding sites for alpha-dystroglycan and heparin. EMBO J. 19, 1432–1440.

26. Hohenester, E., Tisi, D., Talts, J.F., and Timpl, R. (1999). The crystal structure of a laminin G-like module reveals the molecular basis of alpha-dystroglycan binding to laminins, perlecan, and agrin. Mol. Cell 4, 783–792.

27. Steinmetz, A., Vallée, F., Beil, C., Lange, C., Baurin, N., Beninga, J., Capdevila, C., Corvey, C., Dupuy, A., Ferrari, P., et al. (2016). CODV-Ig, a universal bispecific tetravalent and multifunctional immunoglobulin format for medical applications. MAbs 8, 867–878.

28. Armour, K.L., Clark, M.R., Hadley, A.G., and Williamson, L.M. (1999). Recombinant human IgG molecules lacking Fcgamma receptor I binding and monocyte triggering activities. Eur. J. Immunol. 29, 2613–2624.

29. Labrijn, A.F., Meesters, J.I., de Goeij, B.E., van den Bremer, E.T., Neijssen, J., van Kampen, M.D., Strumane, K., Verploegen, S., Kundu, A., Gramer, M.J., et al. (2013). Efficient generation of stable bispecific IgG1 by controlled Fab-arm exchange. Proc. Natl. Acad. Sci. USA *110*, 5145–5150.

30. Goulet, D.R., Orcutt, S.J., Zwolak, A., Rispens, T., Labrijn, A.F., de Jong, R.N., Atkins, W.M., and Chiu, M.L. (2018). Kinetic mechanism of controlled Fab-arm exchange for the formation of bispecific immunoglobulin G1 antibodies. J. Biol. Chem. *293*, 651–661.

31. Vannoy, C.H., Xu, L., Keramaris, E., Lu, P., Xiao, X., and Lu, Q.L. (2014). Adeno-associated virus-mediated overexpression of LARGE rescues α-dystroglycan function in dystrophic mice with mutations in the fukutin-related protein. Hum. Gene Ther. Methods *25*, 187–196.

32. Xu, L., Lu, P.J., Wang, C.H., Keramaris, E., Qiao, C., Xiao, B., Blake, D.J., Xiao, X., and Lu, Q.L. (2013). Adeno-associated virus 9 mediated FKRP gene therapy restores functional glycosylation of α-dystroglycan and improves muscle functions. Mol. Ther *21*, 1832–1840.

33. Yu, M., He, Y., Wang, K., Zhang, P., Zhang, S., and Hu, H. (2013). Adeno-associated viral-mediated LARGE gene therapy rescues the muscular dystrophic phenotype in mouse models of dystroglycanopathy. Hum. Gene Ther. *24*, 317–330.

34. Vannoy, C.H., Xiao, W., Lu, P., Xiao, X., and Lu, Q.L. (2017). Efficacy of gene therapy is dependent on disease progression in dystrophic mice with mutations in the FKRP gene. Mol. Ther. Methods Clin. Dev. *5*, 31–42.

35. Qiao, C., Wang, C.H., Zhao, C., Lu, P., Awano, H., Xiao, B., Li, J., Yuan, Z., Dai, Y., Martin, C.B., Li, J., et al. (2014). Muscle and heart function restoration in a limb girdle muscular dystrophy 2I (LGMD2I) mouse model by systemic FKRP gene delivery. Mol. Ther *22*, 1890–1899.

36. Gicquel, E., Maizonnier, N., Foltz, S.J., Martin, W.J., Bourg, N., Svinartchouk, F., Charton, K., Beedle, A.M., and Richard, I. (2017). AAV-mediated transfer of FKRP shows therapeutic efficacy in a murine model but requires control of gene expression. Hum. Mol. Genet. *26*, 1952–1965.

37. Kotterman, M.A., and Schaffer, D.V. (2014). Engineering adeno-associated viruses for clinical gene therapy. Nat. Rev. Genet. *15*, 445–451.

38. Mitchell, A.M., Nicolson, S.C., Warischalk, J.K., and Samulski, R.J. (2010). AAV's anatomy: roadmap for optimizing vectors for translational success. Curr. Gene Ther. *10*, 319–340.

39. McKee, K.K., Crosson, S.C., Meinen, S., Reinhard, J.R., Rüegg, M.A., and Yurchenco, P.D. (2017). Chimeric protein repair of laminin polymerization ameliorates muscular dystrophy phenotype. J. Clin. Invest. *127*, 1075–1089.

40. Talts, J.F., Andac, Z., Göhring, W., Brancaccio, A., and Timpl, R. (1999). Binding of the G domains of laminin alpha1 and alpha2 chains and perlecan to heparin, sulfatides, alpha-dystroglycan and several extracellular matrix proteins. EMBO J. *18*, 863–870.

41. Talts, J.F., Mann, K., Yamada, Y., and Timpl, R. (1998). Structural analysis and proteolytic processing of recombinant G domain of mouse laminin alpha2 chain. FEBS Lett. *426*, 71–76.

42. Wu, C., Ying, H., Grinnell, C., Bryant, S., Miller, R., Clabbers, A., Bose, S., McCarthy, D., Zhu, R.R., Santora, L., et al. (2007). Simultaneous targeting of multiple disease mediators by a dual-variable-domain immunoglobulin. Nat. Biotechnol. *25*, 1290–1297.

43. Durocher, Y., Perret, S., and Kamen, A. (2002). High-level and high-throughput recombinant protein production by transient transfection of suspension-growing human 293-EBNA1 cells. Nucleic Acids Res. *30*, E9.

44. Li, D., Yue, Y., and Duan, D. (2008). Preservation of muscle force in Mdx3cv mice correlates with low-level expression of a near full-length dystrophin protein. Am. J. Pathol. *172*, 1332–1341.